

## A GEOMETRICAL THEORY FOR $\{111\}$ - $\langle hkl \rangle$ RECRYSTALLISATION TEXTURE FORMATION IN COLD ROLLED IF STEEL

B.J. DUGGAN, Y.Y. TSE and G.L. LIU

Department of Mechanical Engineering, The University of Hong Kong,  
Pokfulam Road, Hong Kong

### Abstract

The introduction of conditional deformation banding into BCC rolling texture modelling has produced a clue as to the origins of the  $\{111\}$ - $\langle hkl \rangle$  texture as develops from the  $\gamma$  fibre material. OIM has revealed that deformation bands are present in many deformed  $\gamma$  grains, which therefore produce the geometrical condition for successful nucleation of rotated  $\langle 111 \rangle$  ND material by either subgrain growth or SIBM. Clearly the roles of solutes and precipitates have to be established in this deformation microstructure.

Key words: IF Steel, Recrystallisation Texture, Deformation Banding, Nucleation Sites

### 1. Introduction

The introduction of deformation banding (DB) into texture modelling by Lee and Duggan (Lee and Duggan, 1993) for the case of intermediate to high stacking fault energy FCC materials produced significant improvement in modelled textures in the rate insensitive regime. The model was refined and successfully predicted the orientations which split into different orientations on straining (Lee *et al.*, 1995). Further improvement was achieved by introducing a conditional energy term which allowed DB to occur progressively with rolling strain (Duggan *et al.*, 1998). Liu *et al.* (1996, 1998) used the essential ideas of DB due to Lee and applied them to the BCC case, and managed to predict BCC rolling textures quite well. A significant drawback is that although DB is a three dimensional phenomenon in which lath-like elements are free to shear as in the pancake model as well as in the rolling plane, it has proved difficult in mathematical terms, to construct a model which works in this way. Instead, in all the models, relaxation in the pancake mode is allowed in the Relaxed Constraints (RC) formulation, and  $e_{23}$  is modelled by DB in a Taylor/Chin framework (Chin, 1969). Thus each orientation in the model becomes two orientations in the sheet plane geometry, either immediately as in the DB case, or with progressive computer straining in the conditional DB (DBC) case. Disregarding DB in longitudinal sections is severe in terms of violation of the observed physics of deformation because DB is obvious in this section at higher strains, and grain fragmentation, its precursor, in the lower strain regime. However, this drawback has lead the authors to different conclusions regarding the origins of  $\{111\}$ - $\langle hkl \rangle$  recrystallisation textures because, in seeking verification of the BCC DB theory,

emphasis has been on the orientations formed in the rolling plane and predicted by the model. The results are significant in terms of nucleation theory.

## 2. Experimental

Commercially supplied hot band of 3-mm thickness, 30 $\mu$ m grain size and composition shown in table 1 was cold rolled 85% in a laboratory mill of 252-mm diameter rolls at 15m/min under homogeneous rolling conditions. The continuous annealing process was simulated with the heating rate in the hundreds of degrees per minute and a furnace temperature of 850°C. Partial annealing experiments were carried out by interrupting the cycle with a rapid quench from the temperature attained. Also, to allow the deformed structure to be examined by channelling contrast and EBSD, a recovery anneal lasting 168 hours at 450°C was done, after which no sign of recrystallisation was detected in either longitudinal or rolling plane sections. Pole figures were determined by X-ray diffraction using the Schulz reflection method and Mo radiation, and conventional processing from 200, 220, 310 and 222 pole figures gave the ODF. OIM was done on a S360 SEM using the HKL software and the ICE program.

**Table 1** Chemical composition of reference material, (mass%)

C	Si	Mn	P	S	Al	Ti	N
0.0019	0.010	0.13	0.014	0.014	0.041	0.046	0.0026

## 2.1 Results

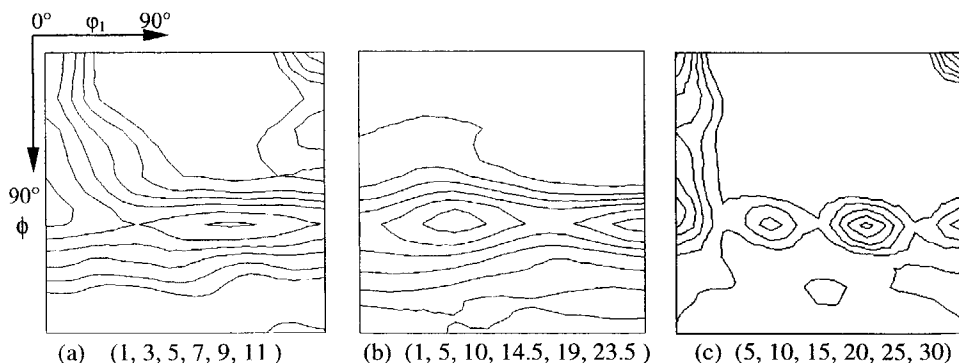


**Figure 1**  $\phi_2 = 45^\circ$  sections of measured and simulated ODFs, (a) 85% cold rolled IF steel, (b) annealed at 850°C, (c) predicted with DBC,  $\sigma = 5\%$

The  $\phi_2 = 45^\circ$  section of the Bunge Euler space is used to represent the full ODF and figure 1 shows the results after cold rolling 85% (a) after complete recrystallisation (b) and (c) after computer simulated rolling 87% following the procedures outlined by Liu *et al.* (1998). The rolling texture is as expected, showing well populated  $\alpha$  and  $\gamma$  fibres, and the recrystallisation texture a strong  $\{111\}\langle hkl \rangle$

texture with a peak at  $\{111\}\langle 112 \rangle$ . The simulated ODF is of peak type in  $\alpha$  and  $\gamma$  fibres after computer rolling 87% and is too strong. The orientations which feed into the  $\alpha$  and  $\gamma$  fibres after 87% computer rolling in the model are shown in figure 2. It is clear that the  $\gamma$  fibre is fed from a spread around the  $\gamma$  fibre (figure 2a) while the  $\alpha$  fibre source is more complex, figure 2b.

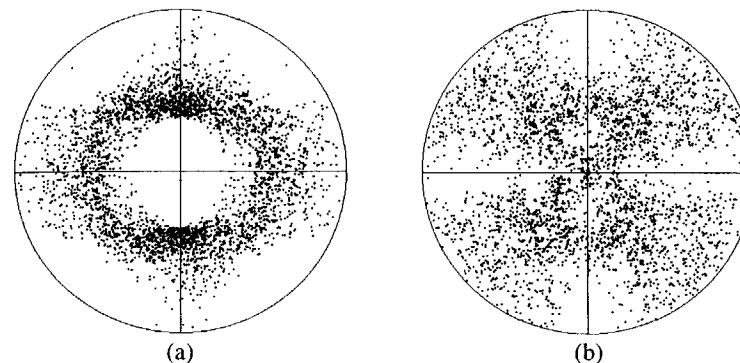


**Figure 2** Initial orientations arriving (a) the  $\gamma$ -fibre and (b) the  $\alpha$ -fibre

Certain orientations which rotated into the  $\gamma$  fibre were then located and followed by increments of 0.05 strain to 87% reduction. A representative set of three such orientation paths are shown in figure 3. In the first case, figure 3a, the orientation rotates to the  $\gamma$  fibre and then splits into two components to give approximately complementary pairs of  $\{111\}\langle 110 \rangle$ ,  $\{111\}\langle 112 \rangle$  and  $\{111\}\langle 110 \rangle$  are predicted to be stable at this level of straining in the computer simulation, but slight rotation about the  $\langle 111 \rangle$  ND produces rotation towards these stable orientations, the particular one being selected by the particular rolling direction, an example is shown in figure 3b. A third kind of rotation is shown in figure 3c in which one component ("1") rotates towards the  $\gamma$  fibre, the other ("2") rotates away towards an important component  $\{114\}\langle 110 \rangle$ .

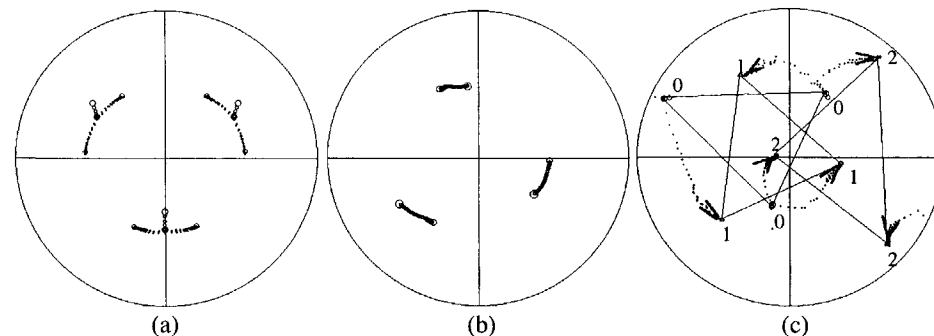


**Figure 3** Rotation of the specific orientations from initial array to the  $\gamma$ -fibre "0" is the original orientation, "1" and "2" are the DB orientations

These predicted orientation splittings were then sought in the rolling plane of electro-polished samples by Orientation Imaging Microscopy (OIM) and, perhaps surprisingly given the two adjustable parameters in the modelling, such geometrical

emphasis has been on the orientations formed in the rolling plane and predicted by the model. The results are significant in terms of nucleation theory.

## 2. Experimental

Commercially supplied hot band of 3-mm thickness, 30 $\mu$ m grain size and composition shown in table 1 was cold rolled 85% in a laboratory mill of 252-mm diameter rolls at 15m/min under homogeneous rolling conditions. The continuous annealing process was simulated with the heating rate in the hundreds of degrees per minute and a furnace temperature of 850°C. Partial annealing experiments were carried out by interrupting the cycle with a rapid quench from the temperature attained. Also, to allow the deformed structure to be examined by channelling contrast and EBSD, a recovery anneal lasting 168 hours at 450°C was done, after which no sign of recrystallisation was detected in either longitudinal or rolling plane sections. Pole figures were determined by X-ray diffraction using the Schulz reflection method and Mo radiation, and conventional processing from 200, 220, 310 and 222 pole figures gave the ODF. OIM was done on a S360 SEM using the HKL software and the ICE program.

**Table 1** Chemical composition of reference material, (mass%)

C	Si	Mn	P	S	Al	Ti	N
0.0019	0.010	0.13	0.014	0.014	0.041	0.046	0.0026

## 2.1 Results

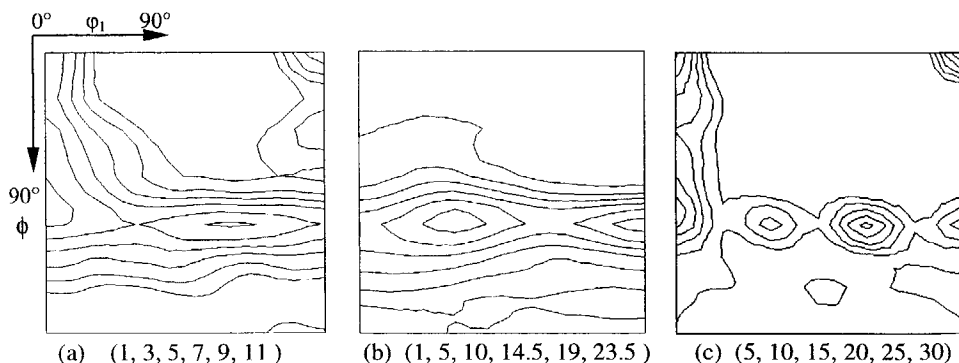


**Figure 1**  $\phi_2 = 45^\circ$  sections of measured and simulated ODFs, (a) 85% cold rolled IF steel, (b) annealed at 850°C, (c) predicted with DBC,  $\sigma = 5\%$

The  $\phi_2 = 45^\circ$  section of the Bunge Euler space is used to represent the full ODF and figure 1 shows the results after cold rolling 85% (a) after complete recrystallisation (b) and (c) after computer simulated rolling 87% following the procedures outlined by Liu *et al.* (1998). The rolling texture is as expected, showing well populated  $\alpha$  and  $\gamma$  fibres, and the recrystallisation texture a strong  $\{111\}\langle hkl \rangle$

texture with a peak at  $\{111\}\langle 112 \rangle$ . The simulated ODF is of peak type in  $\alpha$  and  $\gamma$  fibres after computer rolling 87% and is too strong. The orientations which feed into the  $\alpha$  and  $\gamma$  fibres after 87% computer rolling in the model are shown in figure 2. It is clear that the  $\gamma$  fibre is fed from a spread around the  $\gamma$  fibre (figure 2a) while the  $\alpha$  fibre source is more complex, figure 2b.

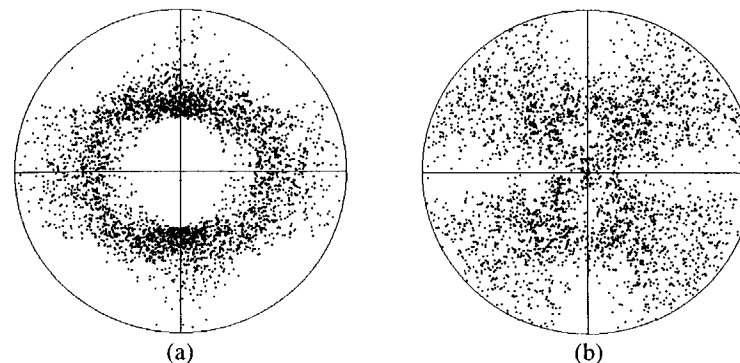


**Figure 2** Initial orientations arriving (a) the  $\gamma$ -fibre and (b) the  $\alpha$ -fibre

Certain orientations which rotated into the  $\gamma$  fibre were then located and followed by increments of 0.05 strain to 87% reduction. A representative set of three such orientation paths are shown in figure 3. In the first case, figure 3a, the orientation rotates to the  $\gamma$  fibre and then splits into two components to give approximately complementary pairs of  $\{111\}\langle 110 \rangle$ ,  $\{111\}\langle 112 \rangle$  and  $\{111\}\langle 110 \rangle$  are predicted to be stable at this level of straining in the computer simulation, but slight rotation about the  $\langle 111 \rangle$  ND produces rotation towards these stable orientations, the particular one being selected by the particular rolling direction, an example is shown in figure 3b. A third kind of rotation is shown in figure 3c in which one component ("1") rotates towards the  $\gamma$  fibre, the other ("2") rotates away towards an important component  $\{114\}\langle 110 \rangle$ .

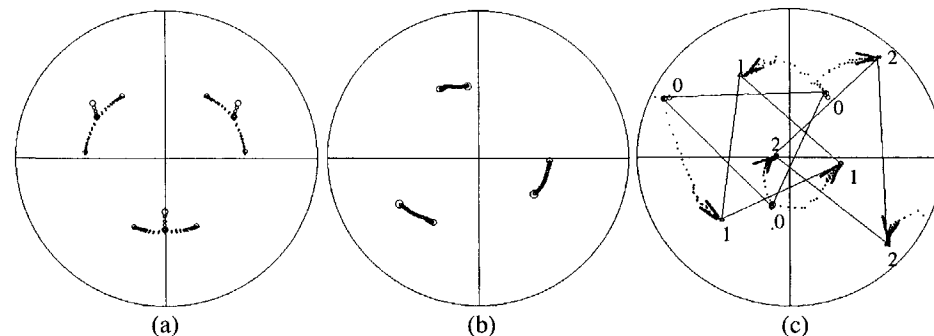


**Figure 3** Rotation of the specific orientations from initial array to the  $\gamma$ -fibre "0" is the original orientation, "1" and "2" are the DB orientations

These predicted orientation splittings were then sought in the rolling plane of electro-polished samples by Orientation Imaging Microscopy (OIM) and, perhaps surprisingly given the two adjustable parameters in the modelling, such geometrical

configurations were discovered without much difficulty in the 85%, cold rolled IF steel in the recovered state. Figure 4a, taken from reference Duggan *et al.* (1999), shows line scans across two contiguous regions having the  $\gamma$  fibre orientation. It is not clear in this micrograph whether these are one or two grains but such a distinction does not matter given the physics involved in DB which can occur several times in one grain. In figure 4a the spread of orientations is  $\sim 30^\circ$  and the material in the central region indicated has the orientation  $\sim \{111\}\langle 110\rangle$  and is surrounded by complementary versions of  $\sim \{111\}\langle 112\rangle$ . These outer regions are those predicted by the model in figure 3a. Presumably the original splitting of orientation occurred at  $\sim \{111\}\langle 112\rangle$  and if some material remained in this orientation this arrangement would resemble precisely that of the transition band described by Hu (1963), and would favour nucleation of recrystallisation. It is unclear which component will dominate in the recrystallisation process, since this depends intimately on several unknown factors to do with the distribution of driving forces. Figure 4c shows a second region divided into two  $\gamma$  fibre components with  $\sim 15^\circ$  misorientation.

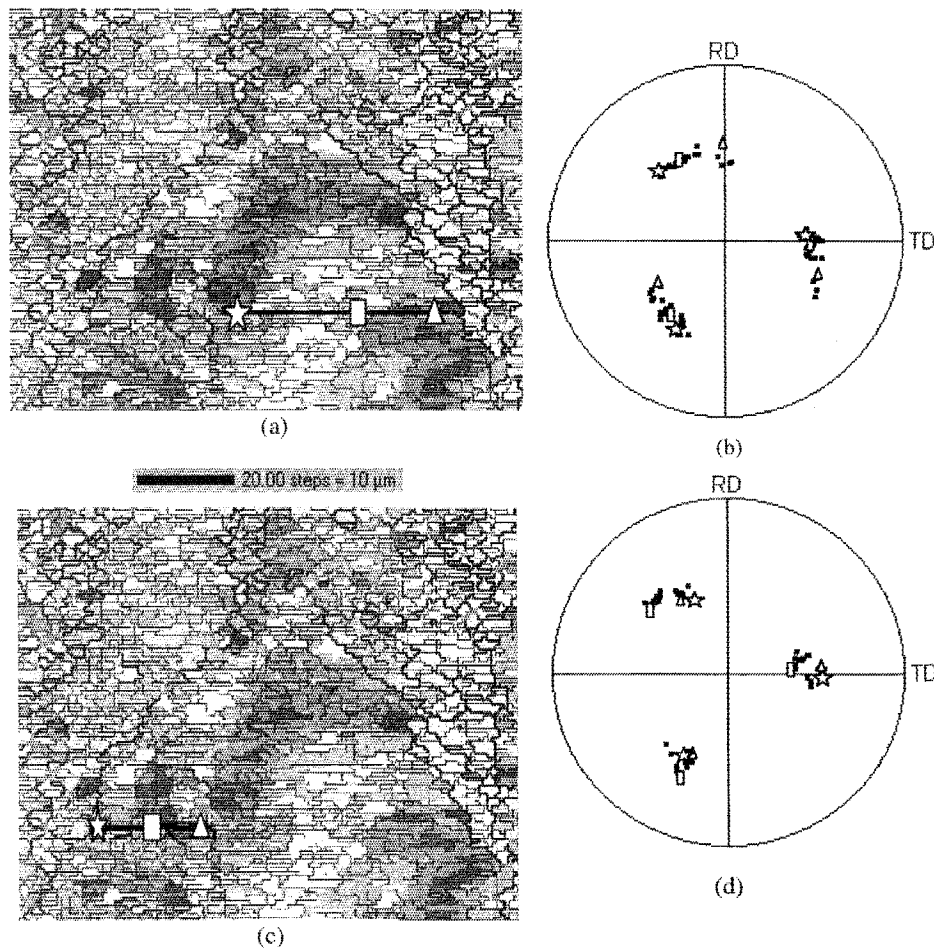


Figure 4 Lattice curvature in annealed IF steel, 450°C and 168hrs, rolling plane

An electro-polished sample was etched lightly to pick out grain boundaries and hence remove some uncertainties in interpretation. The result might not convince sceptics, but an example is shown in figure 5. The width of the grain (if it is indeed a single grain) is 30  $\mu\text{m}$ , precisely the original measured hot band grain size and it can be seen from the channelling contrast image (figure 5a) of the recovered and lightly recrystallised microstructure that a line of subgrains (arrowed) is present curving through the centre of the grain. OIM is shown in figure 5b along with the orientations present in this volume. The orientations are localised into areas, the most prominent being the left side in which a single variant  $\{111\}\langle 112\rangle$  dominates. The right side consists of two components, the complementary  $\{111\}\langle 112\rangle$  to the left side segment, plus volumes spreading from this complement of  $\{111\}\langle 112\rangle$  towards  $\{111\}\langle 110\rangle$ . Such rotations are predicted to occur in DB modelling. Space presents examples of 3c being shown.

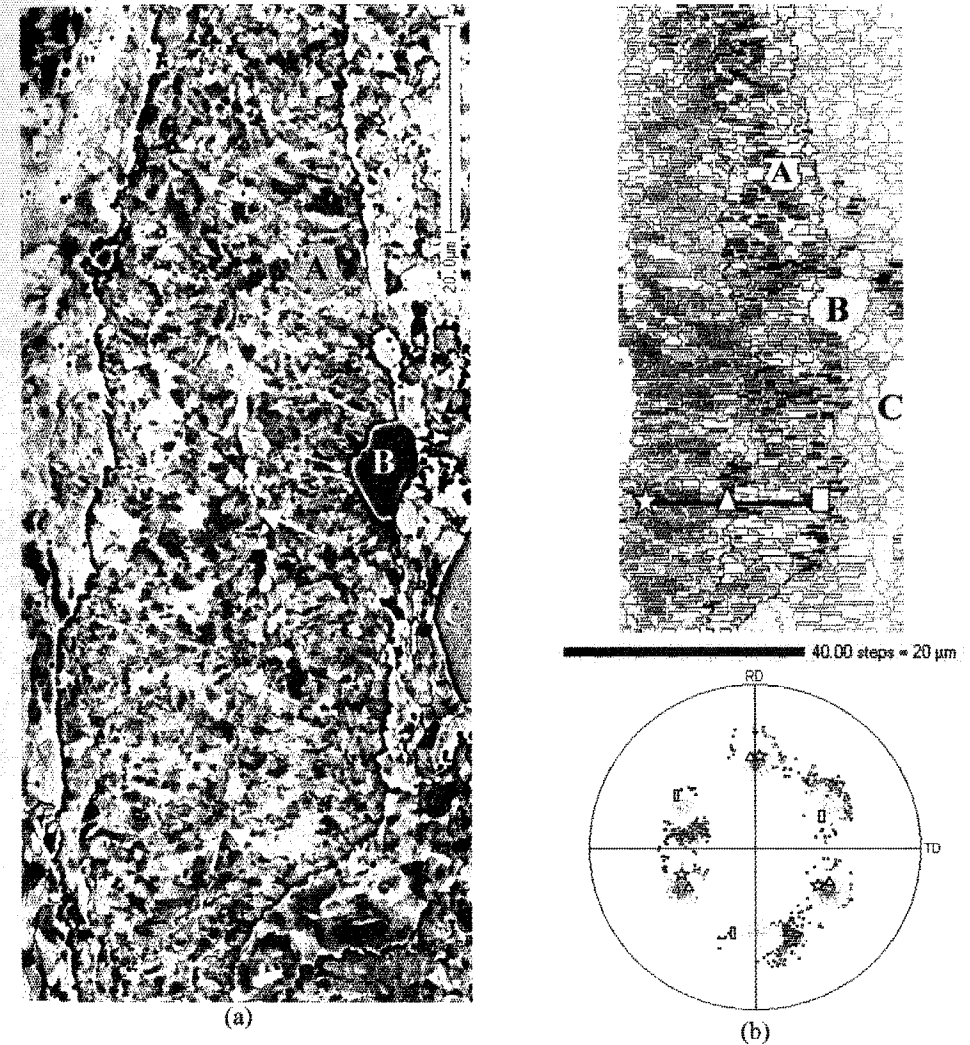


Figure 5 Channelling contrast image (a) and OIM image (b) showing a DB grain

configurations were discovered without much difficulty in the 85%, cold rolled IF steel in the recovered state. Figure 4a, taken from reference Duggan *et al.* (1999), shows line scans across two contiguous regions having the  $\gamma$  fibre orientation. It is not clear in this micrograph whether these are one or two grains but such a distinction does not matter given the physics involved in DB which can occur several times in one grain. In figure 4a the spread of orientations is  $\sim 30^\circ$  and the material in the central region indicated has the orientation  $\sim \{111\}\langle 110\rangle$  and is surrounded by complementary versions of  $\sim \{111\}\langle 112\rangle$ . These outer regions are those predicted by the model in figure 3a. Presumably the original splitting of orientation occurred at  $\sim \{111\}\langle 112\rangle$  and if some material remained in this orientation this arrangement would resemble precisely that of the transition band described by Hu (1963), and would favour nucleation of recrystallisation. It is unclear which component will dominate in the recrystallisation process, since this depends intimately on several unknown factors to do with the distribution of driving forces. Figure 4c shows a second region divided into two  $\gamma$  fibre components with  $\sim 15^\circ$  misorientation.

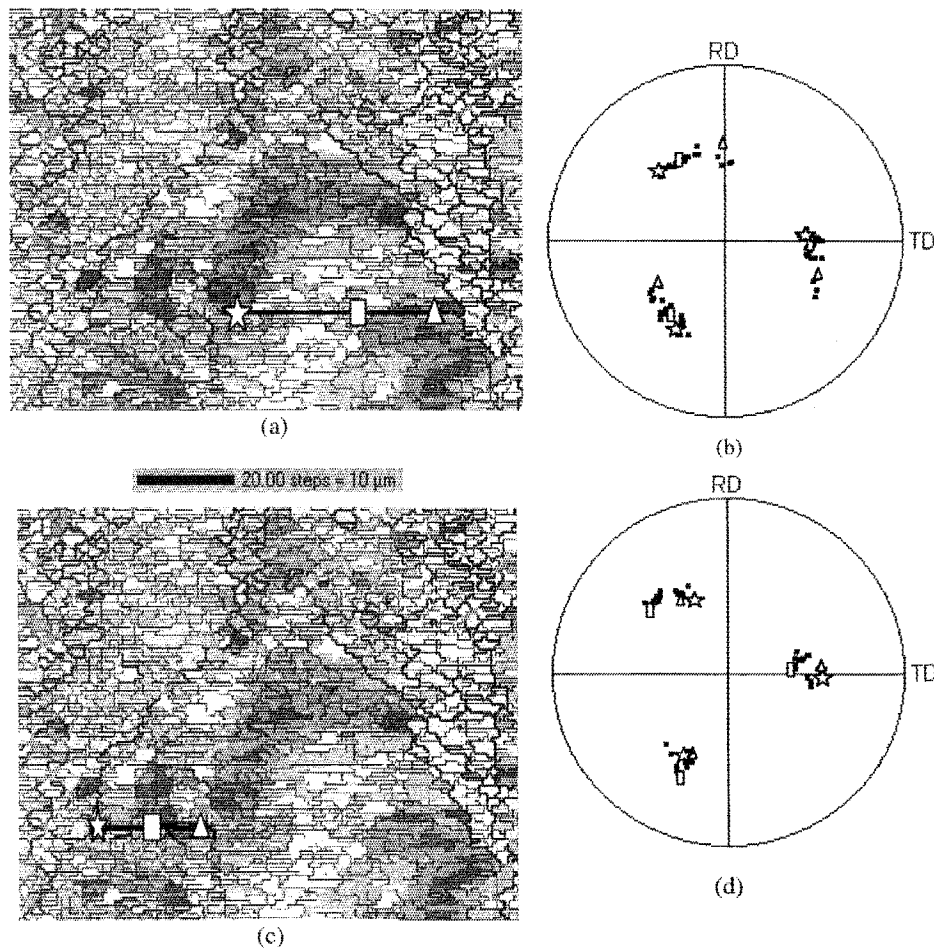


Figure 4 Lattice curvature in annealed IF steel, 450°C and 168hrs, rolling plane

An electro-polished sample was etched lightly to pick out grain boundaries and hence remove some uncertainties in interpretation. The result might not convince sceptics, but an example is shown in figure 5. The width of the grain (if it is indeed a single grain) is 30 $\mu\text{m}$ , precisely the original measured hot band grain size and it can be seen from the channelling contrast image (figure 5a) of the recovered and lightly recrystallised microstructure that a line of subgrains (arrowed) is present curving through the centre of the grain. OIM is shown in figure 5b along with the orientations present in this volume. The orientations are localised into areas, the most prominent being the left side in which a single variant  $\{111\}\langle 112\rangle$  dominates. The right side consists of two components, the complementary  $\{111\}\langle 112\rangle$  to the left side segment, plus volumes spreading from this complement of  $\{111\}\langle 112\rangle$  towards  $\{111\}\langle 110\rangle$ . Such rotations are predicted to occur in DB modelling. Space presents examples of 3c being shown.

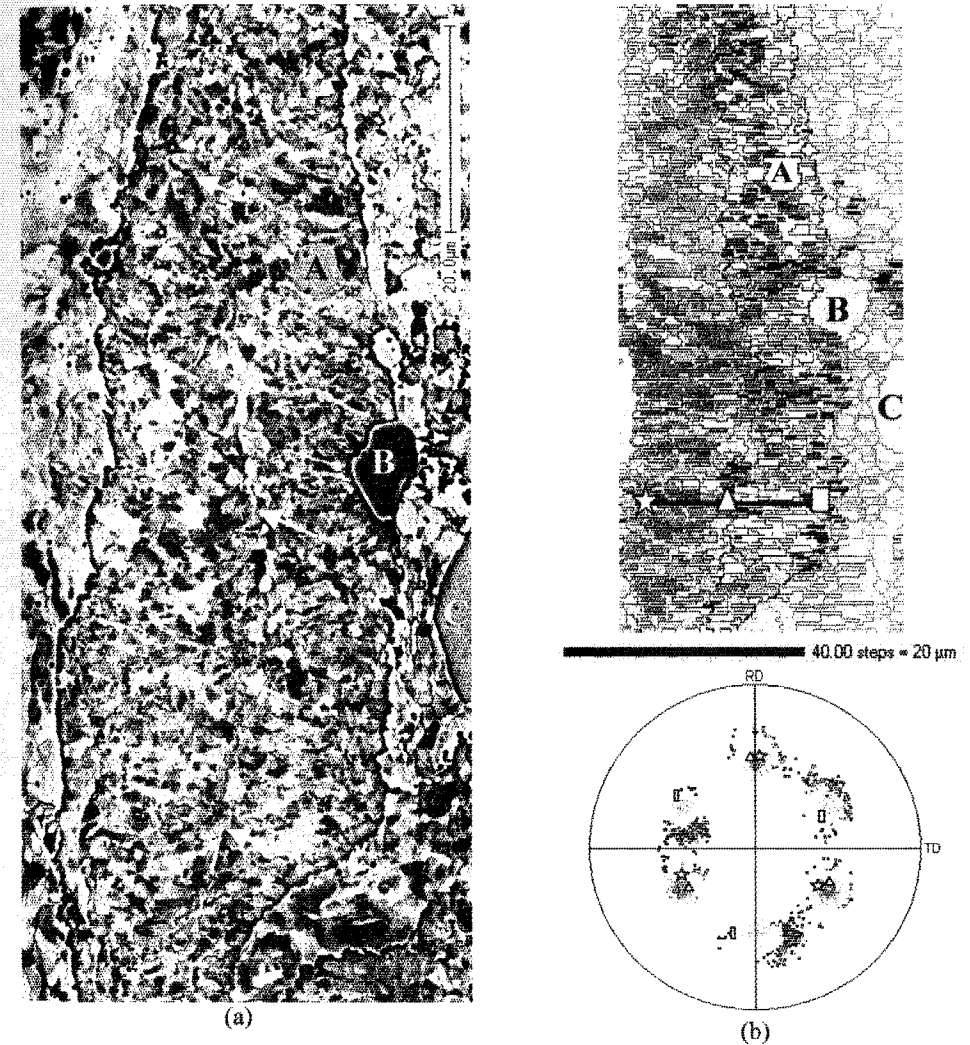


Figure 5 Channelling contrast image (a) and OIM image (b) showing a DB grain

### 3. Summarising Discussion

It seems that all work attempting to link deformed microstructure to recrystallisation processes has, for good reason, concentrated on longitudinal sections for it is here that geometrically necessary dislocation are seen systematically to be associated with regular microstructures. Such microstructure can be associated with nucleation, which must also be a systematic process given the ubiquity of  $\{111\}\langle hkl \rangle$  nucleation. Work done here up to quite recently was not able to improve on work done elsewhere and so explanation was suggested in particle solute effects. It is only by considering the deformation banding process in the one dimensional sense modelled here that lead to surface examination and to the observations reported. Two points can be made: the DB modelling, even in a one dimensional sense, seem to be predictive of the actual orientation splitting that is observed which gives some confidence in the modelling procedure. The second is that the observed orientation splitting in crystals belonging to the  $\gamma$  fibre is capable of providing the necessary geometrical conditions for nucleation. When the gradient is sharp, *i.e.*  $\{111\}\langle hkl \rangle$  is next to  $\{111\}\langle h'k'l \rangle$  and the misorientation is  $\geq 15^\circ$  then nucleation can occur by SIBM. When there is a more gradual orientation gradient, then nucleation is also favoured because subgrain growth need not be too extensive before the necessary misorientation is created for runaway high angle boundary migration. Clearly, this work only provides a geometrical framework for nucleation, neither distribution of driving forces nor the effects of particles or solutes is included and these must also be of critical importance. However, given the three dimensional structure of cold rolled IF steel it is clear that longitudinal sections probably hide more than they reveal, when early recrystallisation processes are being examined either by TEM or SEM.

### Acknowledgements

The authors would like to thank the Croucher Foundation and the Research Grants Council (Hong Kong), for the research grants supporting the work.

### References

- Chin, G. Y. (1969) *Textures in Research and Practice*, p. 236  
 Duggan, B. J., Liu G. L. and Zhang, L. X. (1998) *Materials Science Forum*, Vols. 273–275, p.291  
 Duggan, B. J., Liu, G. L. and Tse, Y. Y. (1999) *Recrystallisation '99*, to be published  
 Hu, H. (1963) *Recovery and Recrystallisation of Metals*, p. 311,  
 Lee, C. S. and Duggan, B. J. (1993) *Acta metall.* Vol. 41, No. 9, p.2691  
 Lee, C. S., Duggan, B. J. and Smallman, R. E. (1995) *Scripta Metall.*, Vol. 33, p. 727  
 Liu, G. L., Duggan, B. J. and Zhang, L. X. (1996) *ICOTOM-11*, p.318  
 Liu, G. L., Duggan, B. J. and Zhang, L. X. (1999) *EPD Congress 1999*, p.1019

### INVESTIGATION OF STEEL SHEET RECRYSTALLISATION TEXTURES WITH A NEW PARAMETER MODEL FOR TEXTURE DESCRIPTION

L. DELANNAY, A. VAN BAEL and P. VAN HOUTTE

Department of Metallurgy and Materials Engineering, Katholieke Universiteit Leuven, Belgium

L. KESTENS and Y. HOUBAERT

Laboratory for Iron and Steelmaking, University of Gent, Belgium

### Abstract

The recrystallisation texture of a steel sheet is influenced by the cold-rolling reduction prior to annealing. In order to study this relationship, textures have been characterised using a new parameter model for texture description in steel sheets. It relies on 25 parameters that characterise the intensity, the "thickness" and the true position of three fibres of the ODF: the classical  $\alpha$ - and  $\gamma$ -fibres and the  $\theta$ -fibre which comprises the "Goss" and "cube" components. For the purpose of this sensitivity study, commercial steel sheet was cold rolled to different reductions varying between 65 and 95% and was annealed afterwards. The experimental ODFs are reproduced using the new parameter model. This allows for an efficient investigation of texture sensitivity based on the 25 relevant parameters. Besides the commonly observed shifts of intensity peaks to more stable crystallographic components, one recognises gradual changes in the position and the "thickness" of the fibres with increasing cold rolling reduction.

Keywords: Quantitative texture analysis, recrystallisation textures, steel sheets

### 1 Introduction

The crystallographic texture present in a cold-rolled and annealed steel sheet is responsible for the anisotropy of the material properties. For example, very slight changes in the Orientation Distribution Function (ODF) can strongly affect planar anisotropy (Delannay et al. 1999a). The optimisation of the sheet texture with regard to its further applications, requires fine-tuning of the rolling and annealing process conditions.

In the present study, we investigate how the level of cold rolling (CR) modifies the ODF obtained after annealing. For this purpose, six experimental textures